Nuclear Engineering and Technology 53 (2021) 3808–3815

Contents lists available at ScienceDirect

Nuclear Engineering and Technology

journal homepage: www.elsevier.com/locate/net

Original Article

Evaluation of photon radiation attenuation and buildup factors for energy absorption and exposure in some soils using EPICS2017 library

F.C. Hila [a, b, *], A.M.V. Javier-Hila [b], M.I. Sayyed [c, d], A. Asuncion-Astronomo [b], G.P. Dicen [b], J.F.M. Jecong [b], N.R.D. Guillermo [b], A.V. Amorsolo Jr. [e]

[a] Materials Science and Engineering Program, College of Engineering, University of the Philippines Diliman, Quezon City, 1101, Metro Manila, Philippines
[b] Department of Science and Technology - Philippine Nuclear Research Institute, Commonwealth Avenue, Diliman, Quezon City, 1101, Metro Manila, Philippines
[c] Department of Nuclear Medicine Research, Institute for Research and Medical Consultations (IRMC), Imam Abdulrahman bin Faisal University (IAU), P.O. Box 1982, Dammam, 31441, Saudi Arabia
[d] Department of physics, Faculty of Science, Isra University, Amman – Jordan
[e] Department of Mining, Metallurgical and Materials Engineering, College of Engineering, University of the Philippines Diliman, Quezon City, 1101, Metro Manila, Philippines

ARTICLE INFO

Article history:
Received 30 November 2020
Received in revised form
3 May 2021
Accepted 23 May 2021
Available online 29 May 2021

Keywords:
EABF
EBF
EPICS2017
Gamma ray
Mass attenuation coefficients
SiO2

ABSTRACT

In this paper, the EPICS2017 photoatomic database was used to evaluate the photon mass attenuation coefficients and buildup factors of soils collected at different depths in the Philippine islands. The extraction and interpolation of the library was accomplished at the recommended linear-linear scales to obtain the incoherent and total cross section and mass attenuation coefficient. The buildup factors were evaluated using the G-P fitting method in ANSI/ANS-6.4.3. An agreement was achieved between XCOM, MCNP5, and EPICS2017 for the calculated mass attenuation coefficient values. The buildup factors were reported at several penetration depths within the standard energy grid. The highest values of both buildup factor classifications were found in the energy range between 100 and 400 keV where incoherent scattering interaction probabilities are predominant, and least at the region of predominant photoionization events. The buildup factors were examined as a function of different soil silica contents. The soil samples with larger silica concentrations were found to have higher buildup factor values and hence lower shielding characteristics, while conversely, those with the least silica contents have increased shielding characteristics brought by the increased proportions of the abundant heavier oxides.

1. Introduction

Ionizing photon radiation is used for numerous medical and industrial applications and scientific research and developments. X-rays and gamma rays have high energies corresponding to small wavelengths that are comparable to atomic spacing; this makes them vital for probing the atomic structures of materials [1]. However, these photons can also cause alterations in the physical, chemical, thermal, optical, and electrical properties of a material. This may be beneficial or detrimental towards the properties of the irradiated medium [2–6]. Furthermore, the high energies of these photons can directly or indirectly cause breaks in DNA molecules [7]. Radiation shielding materials are hence continuously developed and characterized to advance the safe applications of this radiation [8–12].

Radiation shielding properties of several classes of materials have been studied towards the applications of ionizing radiation. Soil is regarded as a cheap, common, and efficient shielding media due to its nature as the abundant solid matter in Earth's crust [13–15]. The photon attenuation characteristics of soils are also useful in techniques such as soil bulk density measurement, particle size analysis, and self-absorption correction in gamma spectrometry of geological samples [16–20]. Several studies have evaluated the photon attenuation characteristics of soils of different origins [13,21–27].

The mass attenuation coefficient (or cross section) is a vital parameter that can describe the diffusion of the photons within a

* Corresponding author. Materials Science and Engineering Program, College of Engineering, University of the Philippines Diliman, Quezon City, 1101, Metro Manila, Philippines.
E-mail address: fchila@pnri.dost.gov.ph (F.C. Hila).

https://doi.org/10.1016/j.net.2021.05.030

material. Experimental and theoretical methods are typically used to evaluate the mass attenuation coefficient for a multi-element material. The most widely used method is by the XCOM-NIST [28,29] web program. On the other hand, several researchers have otherwise extracted mass attenuation coefficients by Monte Carlo simulation codes (e.g., MCNP5, PHITS, Geant4) commonly based on EPDL97 [23,30–37]. Evaluation of mass attenuation coefficients (partials and total) are important as these are used to derive the other significant shielding parameters. In radiation dosimetry and shielding, the buildup factors are derived from the partial mass attenuation coefficients of photon scattering. Buildup factors are important since the contribution of scattered photons towards absorbed doses becomes much higher with increasing penetration depth into the material. Buildup factors have been extensively evaluated for several media, including different construction and foundation materials such as classes of rocks, bricks, and ashes [38–42]. This quantity can be effectively estimated using the G-P fitting method introduced and modified by Harima [43–45]. However, to evaluate buildup factors by the G-P method, the incoherent and total mass attenuation coefficients or cross sections are vital.

The Electron-Photon Interaction Cross Sections 2017 (EPICS2017) [46] is a collective library containing the latest photoatomic data and cross sections for photon transport. This collection supersedes existing libraries embedded in major Monte Carlo codes. EPICS2017 is the official ENDF/B-VIII electron and photon data [47]. It was released by IAEA-NDS in the ENDL and ENDF data formats. An important change towards EPICS2017 is its linearization or its quality as a linearly interpolated library. Since it can be interpolated via linear-linear scales, this library is considered more user-friendly as compared to previous superseded transport libraries. It can be employed more easily towards photon shielding research as well as photon transport code developments. Most importantly, EPICS2017 also contains improved binding energies and cross sections.

This study uses the EPICS2017 database released by the IAEA to evaluate photon attenuation and buildup in several soil samples collected from the Philippine islands. The soil samples were taken at two different sampling depths in five distinct sites. The EPICS2017 was used *via* interpolation of the database to derive the partial and total cross sections and the total mass attenuation coefficients. The recommended linear-linear scheme of the library was employed for all partial cross sections. Buildup factors for energy absorption and exposure were obtained using the G-P fitting method at different penetration depths in the standard energy grid of ANSI/ANS-6.4.3 [48]. Subsequently, each buildup factor parameter was evaluated as a function of silica content, at varying energies and depths. At present, the EPICS2017 is the most recent photon-electron library for photon transport applications. Hence, the application of this library for radiation shielding characterizations would result in favorable evaluations compared to conventional theoretical methods.

2. Materials and methods

2.1. Theoretical background

The two major classifications of the buildup factors are (a) the energy absorption buildup factor (EABF) and (b) the exposure buildup factor (EBF), where the quantities of interest are absorbed energy and exposure, respectively [49]. For both classifications, the ANSI/ANS-6.4.3 contains a compilation of G-P fitting parameters for 23 elements (Be, B, C, N, O, Na, Mg, Al, Si, P, S, Ar, K, Ca, Fe, Cu, Mo, Sn, La, Gd, W, Pb and U) in the photon energy range between 0.015 and 15 MeV, for penetration depths up to 40 mfp.

There are three steps for obtaining the EABF or EBF using the G-P method with ANSI/ANS-6.4.3 database: (*i*) calculation of the material's equivalent atomic number Z_{eq}, (*ii*) calculation of the material's G-P fitting parameters (a, b, c, d, and X_k), and (*iii*) estimation of EABF and EBF by the calculated quantities. The energy-dependent Z_{eq} is based on the ratio of the material's incoherent scattering probability and is obtained by Equation (1), where R is the ratio of the μ/ρ for incoherent scattering and μ/ρ for total attenuation without coherent scattering. The R_1 and R_2 are ratios for the two successive elements that have atomic numbers Z_1 and Z_2. Both R_1 and R_2 are chosen such that R of the material lies in-between.

$$Z_{eq} = \frac{Z_1(\log R_2 - \log R) + Z_2(\log R - \log R_1)}{\log R_2 - \log R_1} \tag{1}$$

For calculating the G-P fitting parameters of the material, the database in ANSI/ANS-6.4.3 are used through Equation (2), where F denotes each of the material's five fitting parameters, and F_1 and F_2 are the tabulated elemental parameters in ANSI/ANS-6.4.3 with atomic numbers Z_1 and Z_2.

$$F = \frac{F_1(\log Z_2 - \log Z_{eq}) + F_2(\log Z_{eq} - \log Z_1)}{\log Z_2 - \log Z_1} \tag{2}$$

Subsequently, the buildup factors (EABF or EBF) are then estimated using Equation (3) or (4). The term K represents the photon dose multiplication and change in the shape of the spectrum from that at 1 mfp. It is calculated using the solved G-P fitting parameters through Equation (5).

$$B(E,x) = 1 + \frac{(b-1)(K^x - 1)}{K - 1} \qquad \text{for } K \neq 1 \tag{3}$$

$$B(E,x) = 1 + (b-1)x \qquad \text{for } K = 1 \tag{4}$$

$$K(E,x) = cx^a + d\frac{\tanh\left(\frac{x}{X_k} - 2\right) - \tanh(-2)}{1 - \tanh(-2)} \qquad \text{for } x \leq 40 \text{ mfp} \tag{5}$$

2.2. Soil sampling and composition

Mangrove forest soils were previously collected and characterized in the previous studies of the authors [33,50]. The collection areas include the Philippine provinces in Cebu (in Kodia), Palawan (in Bogtong and Calauit), and Zambales (in Masinloc and Subic). For every site, two sampling depths were made and categorized as *surface* at 0–40 cm and *subsurface* at 40–100 cm sampling depth [33]. An exception to this was for the Kodia site which had a shallow soil layer and hence subsurface depth at this site was only 40–70 cm. The elemental compositions of the soils were taken from Hila et al. [33] and are summarized in Table 1.

2.3. EPICS2017 extraction and interpolation

The latest evaluated cross section library for electrons and photons was used in this work and is called EPICS2017 [46,51]. This was released in 2018 by IAEA-NDS as part of the ENDF/B-VIII [47]. EPICS2017 library is linear-linear interpolable as compared to its predecessors. The linearization was brought about by increasing the size of data points within the photon library. On the other hand, the electron library does not require an increase in data points [51]. The EPICS2017 has new binding energies and therefore new photoionization cross sections.

Table 1
Elemental content (%wt) of Philippine soils found in mangrove forests at different locations and depths [33].

Elements	Bogtong		Calauit		Kodia		Masinloc		Subic	
	Surface (0 −40)	Sub-surface (40 −100)	Surface (0 −40)	Sub-surface (40 −100)	Surface (0 −40)	Sub-surface (40 −75)	Surface (0 −40)	Sub-surface (40 −100)	Surface (0 −40)	Sub-surface (40 −100)
O (8)	51.3	51.2	51.8	50.6	44.2	44.5	48.0	47.2	47.0	44.5
Mg (12)	2.57	2.13	1.69	2.52	3.65	3.70	4.68	4.82	3.88	3.40
Al (13)	4.02	4.20	3.67	5.99	9.22	8.40	8.19	8.08	12.0	12.6
Si (14)	30.1	32.2	39.0	34.4	16.3	14.1	25.8	22.5	24.2	19.3
P (15)	0.02	0.02	<0.01	<0.01	<0.01	0.06	0.03	0.04	0.05	0.03
S (16)	5.48	4.00	1.13	1.08	3.62	5.24	2.49	3.20	1.05	0.84
Ca (20)	0.09	0.02	<0.01	<0.01	13.8	12.6	4.56	4.43	2.46	1.49
Ti (22)	3.61	3.51	1.44	2.95	2.80	4.93	1.44	4.01	0.68	2.65
Mn (25)	0.02	0.02	0.02	0.02	0.03	0.02	0.02	0.02	0.02	0.01
Fe (26)	2.61	2.48	1.08	2.15	5.68	5.94	4.28	5.10	8.03	13.9
Sr (38)	0.02	0.02	<0.01	0.02	0.07	0.06	0.06	0.07	0.08	0.09
Zr (40)	0.18	0.18	0.17	0.25	0.53	0.42	0.47	0.46	0.58	1.00

The data library was collected in ENDF-6 [52] data format from the IAEA-NDS website and interpolated in the relevant photon energies. A short snippet of the EPICS2017 in ENDF-6 format is shown in Fig. 1. This is a snippet for the element Si (Z = 14) that is one of the most abundant elements in common geological samples. The colored headers (Energy, Cross Section, Z, and Type) have been inserted for visual purposes. In this Figure, the energy is in unit eV while the cross section is in unit barns. There are three paired columns of energies and cross section values. These columns are read starting from the left. After the sixth column, the element number and data type are inscribed. For the element number in yellow text, the digits 1400 is for Si (Z = 14) and this continues with 1500 for P (Z = 15), and so on. To the right of these digits, one will find the type of data for these cross sections. A summary of several partial cross sections in EPICS2017 is shown in Table 2. Referring to the snippet, the data type reads 23,502, hence these data are for cross sections of the coherent scattering interaction.

The partial cross sections relevant to buildup factors were interpolated in this work. The total atomic cross section was the sum of photoelectric, incoherent, and pair productions. The interpolation scheme for the entire EPICS2017 is linear-linear, hence this scheme was followed in this work. To facilitate interpolations, it was convenient to store the cross sections in a programming language or a spreadsheet such as that described in Hila et al. [53]. For this present work, a program was written in the C# language.

3. Results and discussion

This study evaluated the photon attenuation and buildup factors of sampled soils from the Philippine islands. The new EPICS2017 photoatomic library of IAEA was used *via* interpolation. The mass attenuation coefficients of the soils evaluated from EPICS2017 are described in Table 3. These show comparative values from XCOM and from MCNP5 based results described in Hila et al. [33]. The last column shows the experimental values of other soils reported in literature for other countries. These values indicate an agreement between both theoretical methods, which are found to be within the range of previous experimental evaluations. The comparison among XCOM, MCNP5 (ENDF/B-VI.8), and EPICS2017 (ENDF/B-VIII) showed that the deviations were the largest in the lower energy region. It is important to reiterate that EPICS2017 has new binding energies and hence new photoelectric cross sections as compared to its predecessors (i.e., EPICS2014, EPDL97, EPDL89). Several predecessors of EPICS2017 are widely used in Monte Carlo codes. For instance, EPDL97 is embedded within MCNP5, PHITS, FLUKA, and many others. Hence, mass attenuation coefficient values derived using EPICS2017 library-based interpolations generally supersede those obtained *via* current available Monte Carlo codes.

Table 2
Several types of MF/MT numbers in EPICS2017 and descriptions.

MF/MT	Description
23/502	Coherent scattering cross-sections
23/504	Incoherent scattering cross-sections
23/515	Pair production cross-sections, Electron field
23/517	Pair production cross-sections, Nuclear field
23/534 to 23/570	Photoionization cross sections, Each subshell

A sample of interpolated soil mass attenuation coefficients in a wide energy range using EPICS2017 is illustrated in Fig. 2. This was for the composition at the Subic surface (Table 1), where the composition served as a considerable average. This was taken at a fine energy grid which considers the X-ray absorption edges covered. It is shown in Fig. 2 that the photoelectric effect is the dominant type of interaction in low energies between 1 and 50 keV. Directly afterwards, incoherent scattering becomes the predominant type of interaction for the moderate energy region. Subsequently, the pair production process in the nuclear field becomes

EPICS2017: 14-Si in ENDF-6 format

```
(Line 0001)   14-Si 2017 Evaluated Photon Data Library (EPDL) by D.E. Cullen  2017 0  0    0
(Line 0002)  14000.0000 27.8447000         -1          0          0          31400 1451    1
…
…
…              Energy     Cross Section    Energy     Cross Section    Energy     Cross Section  Z  Type
(Line 2340)  1.00000000 5.21985E-5 1.12500000 8.40695E-5 1.26562500 1.35600E-4 1400 23502    4
(Line 2341)  1.42382813 2.19130E-4 1.60180664 3.54971E-4 1.80203247 5.76809E-4 1400 23502    5
(Line 2342)  2.02728653 9.41041E-4 2.28069735 .001543259 2.56578451 .002548068 1400 23502    6
…
```

Fig. 1. Snippet of Z = 14 of EPICS2017 in ENDF-6 format.

Table 3
Mass attenuation coefficients (cm^2g^{-1}) of Philippine soils obtained by EPICS2017, XCOM, and MCNP5 [33], with experiments from literature.

Energy (keV)	Bogtong Surface (0–40)			Bogtong Sub-surface (40–100)			Calauit Surface (0–40)			Calauit Sub-surface (40–100)		
	EPICS2017	MCNP5	XCOM	EPICS2017	MCNP5	XCOM	EPICS2017	MCNP5	XCOM	EPICS2017	MCNP5	XCOM
59.5	0.3056	0.3047	0.3050	0.3026	0.3019	0.3021	0.2768	0.2761	0.2764	0.2966	0.2958	0.2961
81.0	0.2122	0.2116	0.2119	0.2110	0.2105	0.2108	0.2009	0.2004	0.2007	0.2086	0.2081	0.2084
88.0	0.1970	0.1965	0.1969	0.1961	0.1956	0.1961	0.1882	0.1878	0.1883	0.1942	0.1937	0.1942
122	0.1583	0.1579	0.1582	0.1579	0.1576	0.1579	0.1552	0.1549	0.1552	0.1572	0.1569	0.1572
303	0.1069	0.1067	0.1070	0.1069	0.1067	0.1069	0.1070	0.1067	0.1070	0.1069	0.1066	0.1069
356	0.1001	0.0999	0.1002	0.1001	0.0999	0.1002	0.1002	0.1000	0.1003	0.1000	0.0998	0.1001
662	0.0768	0.0766	0.0769	0.0768	0.0766	0.0769	0.0770	0.0768	0.0771	0.0768	0.0766	0.0769
835	0.0690	0.0688	0.0690	0.0690	0.0688	0.0691	0.0691	0.0690	0.0692	0.0689	0.0688	0.0690
1173	0.0583	0.0582	0.0584	0.0584	0.0582	0.0585	0.0585	0.0584	0.0586	0.0583	0.0582	0.0584
1332	0.0547	0.0546	0.0548	0.0547	0.0546	0.0548	0.0548	0.0547	0.0549	0.0547	0.0546	0.0548
Energy (keV)	Kodia Surface (0–40)			Kodia Sub-surface (40–75)			Masinloc Surface (0–40)			Masinloc Sub-surface (40–100)		
	EPICS2017	MCNP5	XCOM	EPICS2017	MCNP5	XCOM	EPICS2017	MCNP5	XCOM	EPICS2017	MCNP5	XCOM
59.5	0.4016	0.4004	0.4006	0.4021	0.4009	0.4011	0.3379	0.3369	0.3372	0.3580	0.3569	0.3572
81.0	0.2507	0.2500	0.2503	0.2505	0.2498	0.2501	0.2252	0.2246	0.2250	0.2331	0.2324	0.2328
88.0	0.2270	0.2264	0.2269	0.2268	0.2262	0.2266	0.2072	0.2067	0.2071	0.2132	0.2127	0.2131
122	0.1716	0.1712	0.1715	0.1693	0.1688	0.1692	0.1626	0.1622	0.1625	0.1647	0.1643	0.1647
303	0.1077	0.1074	0.1077	0.1073	0.1070	0.1073	0.1071	0.1069	0.1072	0.1071	0.1068	0.1071
356	0.1005	0.1002	0.1006	0.1002	0.1000	0.1003	0.1002	0.1000	0.1003	0.1000	0.0998	0.1002
662	0.0767	0.0765	0.0767	0.0765	0.0764	0.0766	0.0767	0.0766	0.0768	0.0766	0.0764	0.0766
835	0.0688	0.0686	0.0689	0.0687	0.0685	0.0688	0.0689	0.0687	0.0690	0.0687	0.0686	0.0688
1173	0.0582	0.0580	0.0583	0.0581	0.0580	0.0582	0.0583	0.0581	0.0584	0.0581	0.0580	0.0582
1332	0.0545	0.0544	0.0546	0.0544	0.0543	0.0545	0.0546	0.0545	0.0547	0.0545	0.0544	0.0546

Energy (keV)	Subic Surface (0–40)			Subic Sub-surface (40–100)			Experiments in literature
	EPICS2017	MCNP5	XCOM	EPICS2017	MCNP5	XCOM	
59.5	0.3635	0.3625	0.3627	0.4421	0.4409	0.4411	0.239–0.322[a]; 0.3562–0.3793[b]; 0.243[c]
81.0	0.2362	0.2356	0.2359	0.2676	0.2668	0.2671	0.181–0.202[a]
88.0	0.2157	0.2151	0.2156	0.2400	0.2394	0.2398	0.173–0.189[a]
122	0.1651	0.1647	0.1651	0.1740	0.1735	0.1738	0.140[f]
303	0.1070	0.1067	0.1070	0.1071	0.1068	0.1071	0.098–0.106[e]
356	0.1000	0.0998	0.1001	0.0999	0.0997	0.1000	0.135[c]; 0.082–0.096[d]; 0.091–0.098[e]
662	0.0765	0.0764	0.0766	0.0761	0.0760	0.0762	0.0708–0.0773[b]; 0.113[c]; 0.064–0.074[d]
835	0.0687	0.0685	0.0688	0.0683	0.0682	0.0684	0.0700[f]
1173	0.0581	0.0580	0.0582	0.0578	0.0576	0.0579	0.092[c]; 0.047–0.054[d]
1332	0.0544	0.0543	0.0545	0.0541	0.0540	0.0542	0.079[c]; 0.042–0.049[d]

[a] Akman et al. [13].
[b] Costa et al. [17].
[c] Taqi et al. [26].
[d] Medhat [57].
[e] Alam et al. [21].
[f] Appoloni & Rios [22].

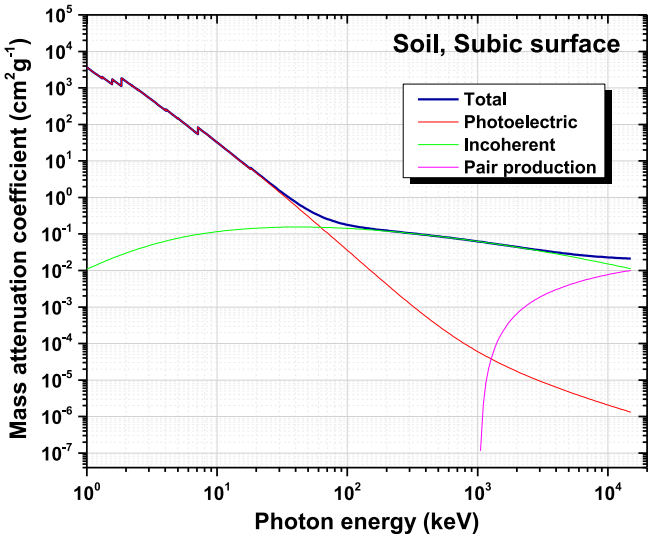

Fig. 2. EPICS2017 based partial and total mass attenuation coefficients in a broad energy range for soil collected from the Subic surface sampling site.

possible at threshold energy of 1.022 MeV and continues with increasing probability. Furthermore, pair production becomes the most probable type of interaction at around 18 MeV for the soils considered. In the photoelectric cross section, the prominent X-ray absorption edges are that of the K-edges of Fe (7.117 keV), Si (1.844 keV) and Al (1.564 keV). This is owing to the abundance of these elements in soils found in Subic as well as in the composition of common soil. Conversely, the K-edges of Zr at 18.002 keV and Sr at 16.108 keV are higher than the K-edge of Fe but were not visible in Fig. 2 because of insignificant amounts of Zr and Sr. The most abundant element in the soils is O, which has its K-edge at 0.538 keV. This K-edge is below the recommended range of use of the EPICS2017 library ($E \geq 1$ keV) and is likewise below the range of XCOM-NIST.

Buildup factors for energy absorption and exposure in the investigated mangrove soils are plotted in Fig. 3. These are given for all soil compositions derived from 5 sampling sites at 2 depths per site (i.e., 0–40 cm and 40–100 cm). Calculations were given at photon penetration depths of 1, 5, 10, 20, and 40 mfp. The results from Fig. 3 revealed that, with increasing penetration depth, there is an increase or cascade in the number of scattered photons propagating within the soil that contributes to the increasing buildup factors. Apparently, the maximum values for both EABF and

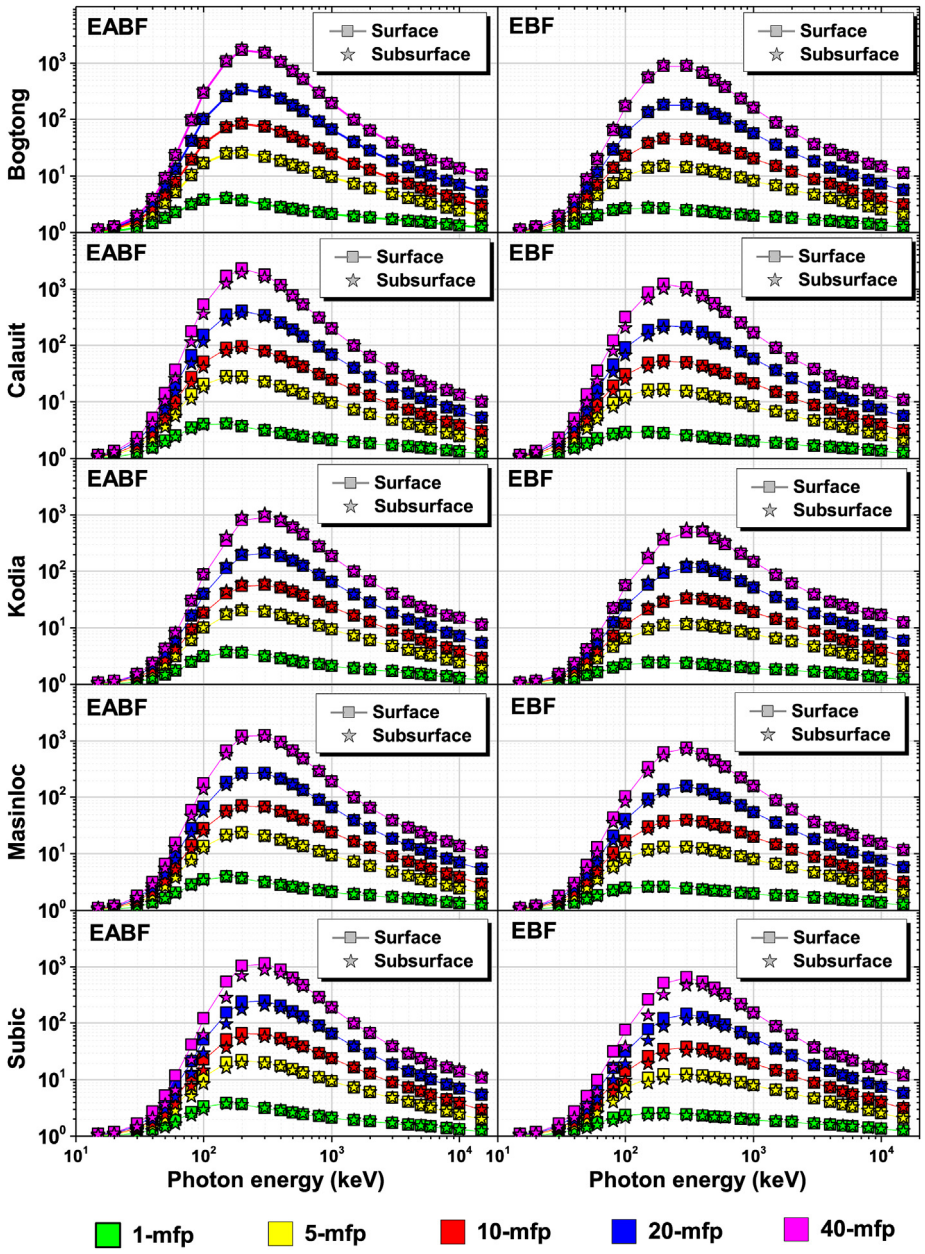

Fig. 3. Soil buildup factors for energy absorption and exposure.

EBF were found in the energy range between 100 and 400 keV depending upon the penetration depth and the chemical compositions. The maximum values were found to be within the range of other materials with similar elemental compositions including silicates, fly-ash, bricks, clays, concretes, and geological samples [39,40,54,55].

Moreover, both buildup factor classifications retain the least values towards the low energy region. The quantities approach unity at 15 keV which is the lower limit of the photon energy range considered. This is due to the large probability of photoelectric absorption interaction that decreases the average photon lifetime within the soil medium. Particularly, photoionization events lead to a reduction of primary photons that otherwise could have undergone scattering. For energies in the order of several keV (~50 keV), the incoherent scattering interaction becomes the predominant mechanism as indicated in Fig. 2. Due to increased scattering beyond the low energy range, there is a substantial increase in buildup factor values within the intermediate energy region, and it is evident from Fig. 3 that EABF and EBF at intermediate energies have skewed trends, where the maximum values for both parameters were found. Beyond the intermediate energy range, pair production in the nuclear field becomes possible and significant and is characterized by an increasing probability with respect to energy. It is important to state that pair production is a type of absorption that affects buildup by decreasing the prevalence of high-energy photons scattering further within the material (soil samples) but leads to the production of electron-positron pairs that may also contribute scattered photons through the generation of X-rays and gamma rays from annihilation.

It is to be noted that the soils in Calauit which have the highest silica content also have the highest EABF and EBF. Silica or silicon oxide (SiO_2) is typically the most abundant component in soil, and

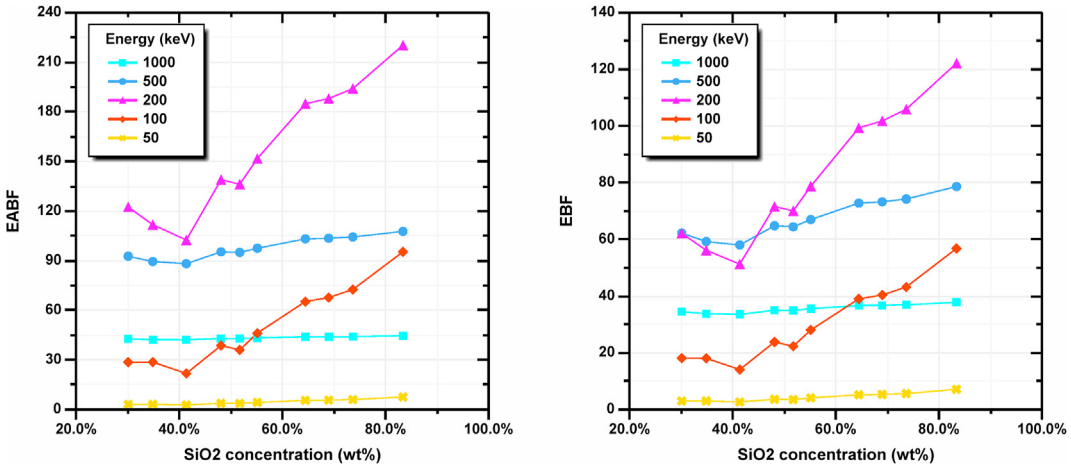

Fig. 4. Buildup factors vs SiO_2 content for soils at several photon energies for 15 mfp depth.

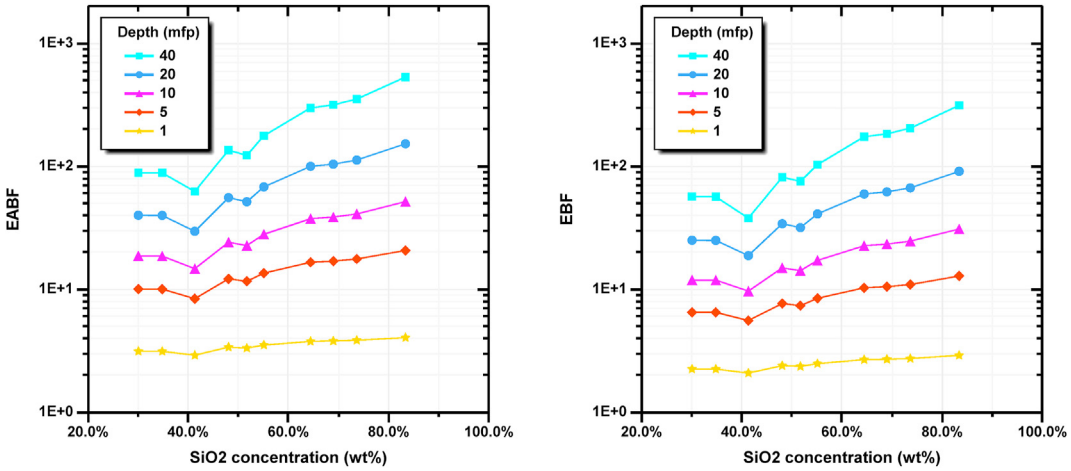

Fig. 5. Buildup factors vs SiO_2 content for soils at several depths for 100 keV photon energy.

one of the lighter compounds of the material. Accordingly, an inverse relationship between silica content and photon shielding capabilities is likely to be present in the soil. The effects of soils' silica concentrations versus mass attenuation coefficients were previously reported in several studies [33,56,57].

The buildup factors were examined as a function of different soil silica contents to evaluate the dependence of the chemical composition on this parameter. Fig. 4 describes the EABF and EBF of soil as a function of silica content at varying photon energies taken at fixed 15 mfp. It indicates that buildup factor values are much smaller at low energies where photoionization cross sections are relatively high. As energy approaches the intermediate region, buildup factors are strongly affected by silica content. These results are supplemented by Fig. 5 where buildup factors for intermediate energy 100 keV photons are plotted at multiple penetration depths. Furthermore, Fig. 4 shows that buildup factors tend to be independent of soil compositions as the starting photon energy approaches 1 MeV.

Since high ratios of silica decrease the proportions of heavier oxides such as iron oxide or aluminum oxide, soils with high silica content were demonstrated to be less capable in terms of shielding against X-ray and gamma ray photons. Consequently, soils with low silica content have increased proportions of heavier oxides and therefore have higher shielding capacities. This is emphasized by their lower buildup factors in the intermediate photon energy range. For these heavier soils, the radiation shielding capacities are dictated by the ratios of the other oxides that are heavier than silica. Iron oxide is the heaviest among the abundant common oxides found in soil. Hence, heavy soils (high iron oxide contents and low silica contents) are expected to have better radiation shielding characteristics.

4. Conclusion

This study evaluated the photon attenuation and buildup factors for energy absorption and exposure using cross sections based on the EPICS2017 photoatomic library. The EPICS2017 is the official ENDF/B-VIII electron-photon data for transport applications. The details of the library extraction and interpolation have been described. The buildup factors were examined as a function of different soil silica contents to evaluate their dependence on chemical compositions. Buildup factors were highest at the photon energy region between 100 and 400 keV wherein incoherent scattering is the predominant mode of interaction, and least at the region of predominant photoionization interactions. Results show increasing buildup factors as a function of silica concentrations, denoting that soils with high silica content are less desirable for gamma photon shielding. Conversely, soils with lower silica

contents have larger quantities of heavier oxides and therefore have lower buildup factors and better overall photon shielding characteristics. Since the EPICS2017 collection is now linearized, this collection may be favorable for shielding characterizations owing to its user-friendly construction; this is especially since the new EPICS2017 contains new binding energies and cross sections.

Declaration of competing interest

The authors declare that they have no known competing financial interests or personal relationships that could have appeared to influence the work reported in this paper.

References

[1] J.D. Brock, M. Sutton, Materials science and X-ray techniques, Mater. Today 11 (2008) 52–55.
[2] G.E.P. Lopez, J.F. Madrid, L.V. Abad, Chromium and cadmium adsorption on radiation-grafted polypropylene copolymers: regeneration, kinetics, and continuous fixed bed column studies, SN Appl. Sci. 2 (3) (2020).
[3] A. Madhu, B. Eraiah, N. Srinatha, Gamma irradiation effects on the structural, thermal and optical properties of samarium doped lanthanum–lead- boro-tellurite glasses, J. Lumin. 221 (2020) 117080.
[4] S. Punia, S.B. Dhull, P. Kunner, S. Rohilla, Effect of γ-radiation on physico-chemical, morphological and thermal characteristics of lotus seed (Nelumbo nucifera) starch, Int. J. Biol. Macromol. 157 (2020) 584–590.
[5] D. Toyen, E. Wimolmala, N. Sombatsompop, T. Markpin, K. Saenboonruang, Sm2O3/UHMWPE composites for radiation shielding applications: mechanical and dielectric properties under gamma irradiation and thermal neutron shielding, Radiat. Phys. Chem. 164 (2019) 108366.
[6] C. Tranquilan-Aranilla, B.J.D. Barba, L.S. Relleve, L.V. Abad, In vivo safety evaluation of granules and dressing hemostatic agents from radiation processed polymeric materials, Philipp. J. Sci. 149 (S1) (2020) 15–26.
[7] C. Von Sonntag, Free-Radical-Induced DNA Damage and its Repair: A Chemical Perspective, Springer-Verlag, Berlin Heidelberg, 2006.
[8] L.A. Escalera-Velasco, J.R. Molina-Contreras, C.G. Hernández-Murillo, H.A. De León-Martínez, H.R. Vega-Carrillo, J.A. Rodríguez-Rodríguez, I.A. López-Salas, Shielding behavior of artisanal bricks against ionizing photons, Appl. Radiat. Isot. 161 (2020).
[9] E. Kavaz, H.O. Tekin, N.Y. Yorgun, Ö.F. Özdemir, M.I. Sayyed, Structural and nuclear radiation shielding properties of bauxite ore doped lithium borate glasses: experimental and Monte Carlo study, Radiat. Phys. Chem. 162 (2019) 187–193.
[10] M.I. Sayyed, K.M. Kaky, M.H.A. Mhareb, A.H. Abdalsalam, N. Almousa, G. Shkoukani, M.A. Bourham, Borate multicomponent of bismuth rich glasses for gamma radiation shielding application, Radiat. Phys. Chem. 161 (2019a) 77–82.
[11] D.K. Gaikwad, M.I. Sayyed, S.S. Obaid, S.A.M. Issa, P.P. Pawar, Gamma ray shielding properties of TeO2-ZnF2-As2O3-Sm2O3 glasses, J. Alloys Compd. 765 (2018) 451–458.
[12] D.K. Gaikwad, M.I. Sayyed, S.N. Botewad, S.S. Obaid, Z.Y. Khattari, U.P. Gawai, F. Afaneh, M.D. Shirshat, P.P. Pawar, Physical, structural, optical investigation and shielding features of tungsten bismuth tellurite based glasses, J. Non-Cryst. Solids 503–504 (2019) 158–168.
[13] F. Akman, V. Turan, M.I. Sayyed, F. Akdemir, M.R. Kaçal, R. Durak, M.H.M. Zaid, Comprehensive study on evaluation of shielding parameters of selected soils by gamma and X-rays transmission in the range 13.94–88.04 keV using WinXCom and FFAST programs, Results Phys 15 (2019) 102751.
[14] G.S. Mudahar, H.S. Sahota, Soil: a radiation shielding material, Int. J. Radiat. Appl. Instrum. Part A 39 (1) (1988a) 21–24.
[15] G.S. Mudahar, H.S. Sahota, Effective atomic number studies in different soils for total photon interaction in the energy region 10-5000 keV, Int. J. Radiat. Appl. Instrum. Part A 39 (12) (1988b) 1251–1254.
[16] M.S. Al-Masri, M. Hasan, A. Al-Hamwi, Y. Amin, A.W. Doubal, Mass attenuation coefficients of soil and sediment samples using gamma energies from 46.5 to 1332 keV, J. Environ. Radioact. 116 (2013) 28–33.
[17] J.C. Costa, J.A.R. Borges, L.F. Pires, Soil bulk density evaluated by gamma-ray attenuation: analysis of system geometry, Soil Tillage Res. 129 (2013) 23–31.
[18] E.A. Elias, O.O.S. Bacchi, K. Reichardt, Alternative soil particle-size analysis by gamma-ray attenuation, Soil Tillage Res. 52 (1–2) (1999) 121–123.
[19] E.A. Elias, A simplified analytical procedure for soil particle-size analysis by gamma-ray attenuation, Comput. Electron. Agric. 42 (3) (2004) 181–184.
[20] L.F. Pires, Soil analysis using nuclear techniques: a literature review of the gamma ray attenuation method, Soil Tillage Res. 184 (2018) 216–234.
[21] M.N. Alam, M.M.H. Miah, M.I. Chowdhury, M. Kamal, S. Ghose, R. Rahman, Attenuation coefficients of soils and some building materials of Bangladesh in the energy range 276-1332 keV, Appl. Radiat. Isot. 54 (6) (2001) 973–976.
[22] C.R. Appoloni, E.A. Rios, Mass attenuation coefficients of Brazilian soils in the range 10-1450 keV, Appl. Radiat. Isot. 45 (3) (1994) 287–291.
[23] M.E. Medhat, N. Demir, U. Akar Tarim, O. Gurler, Calculation of gamma-ray mass attenuation coefficients of some Egyptian soil samples using Monte Carlo methods, Radiat. Eff. Defect Solid 169 (8) (2014) 706–714.
[24] M.E. Medhat, Comprehensive study of photon attenuation through different construction matters by Monte Carlo simulation, Radiat. Phys. Chem. 107 (2015) 65–74.
[25] M.I. Sayyed, F. Akman, V. Turan, A. Araz, Evaluation of radiation absorption capacity of some soil samples, Radiochim. Acta 107 (1) (2019b) 83–93.
[26] A.H. Taqi, Q.A.M. Al Nuaimy, G.A. Karem, Study of the properties of soil in Kirkuk, Iraq, J. Radiat. Res. Appl. Sci. 9 (3) (2016) 259–265.
[27] Q. Zhang, Y. Guo, H. Bai, Y. Gu, Y. Xu, J. Zhao, L. Ge, Y. Peng, J. Liu, Determination of effective atomic numbers and mass attenuation coefficients of samples using in-situ energy-dispersive X-ray fluorescence analysis, X Ray Spectrom. 47 (1) (2017) 4–10.
[28] M.J. Berger, J.H. Hubbell, XCOM: Photon Cross Sections on a Personal Computer. NBSIR 87-3597, National Bureau of Standards, Gaithersburg, MD, 1987, 1987.
[29] M.J. Berger, J.H. Hubbell, S.M. Seltzer, J. Chang, J.S. Coursey, R. Sukumar, D.S. Zucker, K. Olsen, XCOM: Photon Cross Section Database (Version 1.5), National Institute of Standards and Technology, Gaithersburg, MD, 2010. http://physics.nist.gov/xcom [2020, October 24].
[30] R.A.R. Bantan, M.I. Sayyed, K.A. Mahmoud, Y. Al-Hadeethi, Application of experimental measurements, Monte Carlo simulation and theoretical calculation to estimate the gamma ray shielding capacity of various natural rocks, Prog. Nucl. Energy 126 (2020) 103405.
[31] N. Demir, U.A. Tarim, M.A. Popovici, Z.N. Demirci, O. Gurler, I. Akkurt, Investigation of mass attenuation coefficients of water, concrete and bakelite at different energies using the FLUKA Monte Carlo code, J. Radioanal. Nucl. Chem. 298 (2) (2013) 1303–1307.
[32] M.G. Dong, R. El-Mallawany, M.I. Sayyed, H.O. Tekin, Shielding properties of 80TeO2–5TiO2–(15–x) WO3–xAnOm glasses using WinXCom and MCNP5 code, Radiat. Phys. Chem. 141 (2017) 172–178.
[33] F.C. Hila, G.P. Dicen, A.M.V. Javier-Hila, A. Asuncion-Astronomo, N.R.D. Guillermo, R.V. Rallos, I.A. Navarrete, A.V. Amorsolo JR., Determination of photon shielding parameters for soils in mangrove forests, Philipp. J. Sci. 150 (1) (2021) 245–256.
[34] V.P. Singh, S.P. Shirmardi, M.E. Medhat, N.M. Badiger, Determination of mass attenuation coefficient for some polymers using Monte Carlo simulation, Vacuum 119 (2015) 284–288.
[35] B.T. Tonguc, H. Arslan, M.S. Al-Buriahi, Studies on mass attenuation coefficients, effective atomic numbers and electron densities for some biomolecules, Radiat. Phys. Chem. 153 (2018) 86–91.
[36] S.M. Vahabi, M. Bahreinipour, M. Shamsaie Zafarghandi, Determining the mass attenuation coefficients for some polymers using MCNP code: a comparison study, Vacuum 136 (2017) 73–76.
[37] S.S. Obaid, M.I. Sayyed, D.K. Gaikwad, H.O. Tekin, Y. Elmahroug, P.P. Pawar, Photon attenuation coefficients of different rock samples using MCNPX, Geant4 simulation codes and experimental results: a comparison study, Radiat. Eff. Defect Solid 173 (11–12) (2018) 900–914.
[38] S.S. Obaid, M.I. Sayyed, D.K. Gaikwad, P.P. Pawar, Attenuation coefficients and exposure buildup factor of some rocks for gamma ray shielding applications, Radiat. Phys. Chem. 148 (2018) 86–94.
[39] M.I. Sayyed, M.Y. Alzaatreh, M.G. Dong, M.H.M. Zaid, K.A. Matori, H.O. Tekin, A comprehensive study of the energy absorption and exposure buildup factors of different bricks for gamma-rays shielding, Results Phys 7 (2017) 2528–2533.
[40] V.P. Singh, N.M. Badiger, A comprehensive study on gamma-ray exposure build-up factors and fast neutron removal cross sections of fly-ash bricks, J. Ceram. 2013 (2013) 1–13.
[41] H.R. Vega-Carrillo, K.A. Guzman-Garcia, J.A. Rodriguez-Rodriguez, C.A. Juarez-Alvarado, V.P. Singh, H.A. De León-Martinez, Photon and neutron shielding features of quarry tuff, Ann. Nucl. Energy 112 (2018) 411–417.
[42] S.S. Obaid, D.K. Gaikwad, P.P. Pawar, Determination of gamma ray shielding parameters of rocks and concrete, Radiat. Phys. Chem. 144 (2018) 356–360.
[43] Y. Harima, An approximation of gamma-ray buildup factors by modified geometrical progression, Nucl. Sci. Eng. 83 (2) (1983) 299–309.
[44] Y. Harima, H. Hirayama, Detailed behavior of exposure buildup factor in stratified shields for plane-normal and point isotropic sources, including the effects of bremsstrahlung and fluorescent radiation, Nucl. Sci. Eng. 113 (4) (1993) 367–378.
[45] Y. Harima, Y. Sakamoto, S. Tanaka, M. Kawai, Validity of the geometric-progression formula in approximating gamma-ray buildup factors, Nucl. Sci. Eng. 94 (1) (1986) 24–35.
[46] D.E. Cullen, A Survey of Photon Cross Section Data for Use in EPICS2017, IAEA-NDS-225, rev.1, 2018.
[47] D.A. Brown, M.B. Chadwick, R. Capote, A.C. Kahler, A. Trkov, M.W. Herman, Y. Zhu, ENDF/B-VIII.0: the 8th major release of the nuclear reaction data library with CIELO-project cross sections, new standards and thermal scattering data, Nucl. Data Sheets 148 (2018) 1–142.
[48] Ansi/Ans-6.4.3, Gamma Ray Attenuation Coefficient and Buildup Factors for Engineering Materials, American Nuclear Society La Grange Park, IL, 1991.
[49] I.O. Olarinoye, R.I. Odiaga, S. Paul, EXABCal: a program for calculating photon exposure and energy absorption buildup factors, Heliyon 5 (7) (2019), e02017.
[50] G.P. Dicen, I.A. Navarrete, R.V. Rallos, S.G. Salmo, M.C.A. Garcia, The role of reactive iron in long-term carbon sequestration in mangrove sediments, J. Soils Sediments 19 (1) (2019) 501–510.

[51] D.E. Cullen, EPICS2017: April 2019 Status Report, IAEA-NDS-228, rev.1, 2018.
[52] A. Trkov, M. Herman, D.A. Brown, ENDF-6 Formats Manual: Data Formats and Procedures for the Evaluated Nuclear Data Files, ENDF/B-VI and ENDF/B-VII, CSEWG Document ENDF-102, Report BNL-90365-2009 Rev. 2, Brookhaven National Laboratory, 2009.
[53] F.C. Hila, A.V. Amorsolo Jr., A.M.V. Javier-Hila, N.R.D. Guillermo, A simple spreadsheet program for calculating mass attenuation coefficients and shielding parameters based on EPICS2017 and EPDL97 photoatomic libraries, Radiat. Phys. Chem. 177 (2020).
[54] M. Kurudirek, B. Dogan, Y. Özdemir, A.C. Moreira, C.R. Appoloni, Analysis of some Earth, Moon and Mars samples in terms of gamma ray energy absorption buildup factors: penetration depth, weight fraction of constituent elements and photon energy dependence, Radiat. Phys. Chem. 80 (3) (2011) 354–364.
[55] K.S. Mann, T. Korkut, Gamma-ray buildup factors study for deep penetration in some silicates, Ann. Nucl. Energy 51 (2013) 81–93.
[56] U. Akar Tarim, O. Gurler, E.N. Ozmutlu, S. Yalcin, Monte Carlo calculations for gamma-ray mass attenuation coefficients of some soil samples, Ann. Nucl. Energy 58 (2013) 198–201.
[57] M.E. Medhat, Application of gamma-ray transmission method for study the properties of cultivated soil, Ann. Nucl. Energy 40 (1) (2012) 53–59.